Supporting Information

Multifunctional Tissue-Adhesive Cryogel Wound Dressing for Rapid

Nonpressing Surface Hemorrhage and Wound Repair

Meng Li [a], Zhiyi Zhang [a], Yongping Liang [a], Jiahui He [a], Baolin Guo [a, b, *]

[a] *Frontier Institute of Science and Technology, and State Key Laboratory for Mechanical Behavior of Materials, Xi'an Jiaotong University, Xi'an, 710049, China*

[b] *Key Laboratory of Shaanxi Province for Craniofacial Precision Medicine Research, College of Stomatology, Xi'an Jiaotong University, Xi'an 710049, China*

* To whom correspondence should be addressed. Tel: +86-29-83395363. Fax: +86-29-83395131. E-mail: baoling@mail.xjtu.edu.cn

Experiments and methods

Synthesis of quaternized chitosan (QCS)

The quaternized chitosan (QCS) was synthesized according to our previous research.[1] Briefly, chitosan (5g, M_n=100,000-300,000 Da) was evenly dispersed in 180 mL of deionized (DI) water, then glacial acetic acid (900 µL) was added to the dispersion. Subsequently stirring at 55°C until chitosan was completely dissolved, glycidyltrimethylammonium chloride (GTMAC) (1546 µL) was added dropwise to the reaction system under stirring. The molar ratio was 1:2 of chitosan backbone amino groups to GTAMC. Then the mixture was stirred at 55°C for 18 h. After the reaction, undissolved chitosan in the mixture was removed by centrifugation at 4500 rpm for 20 min at room temperature. The supernatant was reduced pressure filtered by Buchner funnel. The filtrate was further purified by precipitation in pre-cooled ethyl alcohol / acetone mixture (1:1, v/v) for three times. Finally, the purified QCS was putted in a vacuum oven to remove the remaining solvent for 3 days at room temperature.

Characterizations

The Fourier transform infrared spectroscopy (FT-IR) spectra of QCS, dopamine hydrochloride, and lyophilized QCS/PDA2.0 cryogel were detected in the range of 4000-600 cm^{-1} on a Nicolet 6700 FT-IR spectrometer (Thermo Scientific Instrument). The spectra were taken at a resolution of 4 cm^{-1} as the average of 32 scans.

The morphologies of freeze-dried cryogels in three different states (original shape, fixed shape, and recovered shape) were observed in a field emission scanning electron microscope (SEM) (FEI Quanta FEG 250) after sprayed gold.

The swelling ratio in water of cryogels were tested at room temperature. The freeze-dried cryogels were placed in DI water, and after swelling equilibrium the weight of full-water cryogels were measured (Ww). Followed that, the original weight (Wo) of cryogels were obtained after freeze-dried. The cryogel's swelling radio (SR) was calculated by the following formula:

$$SR (\%) = (Ww-Wo)/Wo \times 100\%. \tag{S1}$$

Mechanical performance of the cryogels

The compression test and cyclic compression test were used to evaluate the mechanical performance of the cryogels by employing TA rheometer (DHR-2) at room temperature.[2] The cryogels were made into a cylindrical shape with 8 mm diameter and 10 mm height by specific mold. In the compression test, the freeze-dried cryogels were equilibrated in DI water. Then, the full-water cryogels were placed on the platform of TA rheometer compressed to the maximal compression strain up to 80% at a strain speed of 100 µm/s. In the cyclic compression test, the freeze-dried cryogels were equilibrated in DI water. Then, the full-water cryogels were placed on the platform of TA rheometer and enough water was added around the cryogels. The same as the compression test, the full-water cryogels were compressed to the maximal compression strain up to 80% at a strain speed of 100 µm/s and then released to 0% strain with the same speed. The above processes were cycled 10 times.

Shape recovery performance of the cryogels

The shape recovery properties of the cryogels were tested according to the previous method in our article.[2] Briefly, the cryogels were processed into a cylindrical shape

(with original length of 10 mm (L_0)) and freeze-dried. Then, the lyophilized cryogels were compressed to the 90% strain and keep this state for 5 min to make sure the cryogels were compressed completely. The height of compressed cryogels were measured as L_1. Following that, remove the compression and make the cryogels in free load for 5 min to obtain the shape-fixed cryogel. The length of shape-fixed cryogels were recorded as L_2. After that, the shape-fixed cryogels were immersed in DI water or heparinized whole blood to recover by absorbing water or blood. The height of the recovered cryogels were set as L_3, and recovery time of the above two processes were also recorded. All the above tests were repeated for 5 times with different sample and all the results are average. To further evaluate the shape memory behaviors of the cryogels, the fixity ratio and recovery ratio in water or blood were also calculated by the formulas as following:

Maximum compressive strain: $S_m = (L_0 - L_1)/L_0 \times 100\%$ (S2)

Fixed strain: $S_f = (L_0 - L_2)/L_0 \times 100\%$ (S3)

Recovery strain: $S_r = (L_3 - L_2)/L_1 \times 100\%$ (S4)

Strain fixity ratio: $R_f = S_f / S_m \times 100\%$ (S5)

Strain recovery ratio: $R_r = S_r / S_f \times 100\%$ (S6)

Volumetric expansion ratios of the cryogels

The volumetric expansion ratios of the cryogels were the volume ratio of shape-fixed cryogels before immersed in water or blood (V_f) and after recovered by absorbing water or blood (V_r) in the shape memory properties test. The length of shape-fixed cryogels and recovery cryogels were measured as L_2 and L_3, while the bottom diameter of

cylindrical shape-fixed cryogels and recovery cryogels were recorded as D_2 and D_3. The volumetric expansion ratios of the cryogels were calculated by the equation as following:

$$\text{Volumetric expansion ratio} = V_r / V_f = \frac{\left(\frac{D3}{2}\right)^2 \times L3}{\left(\frac{D2}{2}\right)^2 \times L2}. \tag{S7}$$

***In vitro* biocompatibility test of the cryogels**

The *in vitro* biocompatibility of the cryogels were evaluated by cytocompatibility of the cryogels to L929 cells (mouse fibroblast cell line) through two different methods of the direct contact test and the leaching pattern test. The L929 cells were cultivated at 37°C, 5% CO_2, 100% humidity in complete growth medium composed of the dulbecco's modified eagle medium (DMEM) (Gibco) supplemented with 10% fetal bovine serum (Gibco), 1.0×10^5 U/L penicillin (Hyclone) and 100 mg/L streptomycin (Hyclone). L929 cells were seeded in 40-well plate at a density of 7500 cells/well and cultured for 12 h. After that in the direct contact test, all the cylindrical cryogels with the 8 mm diameter were cut into 5 mm length and sterilized by immersed them into 75% alcohol, then introduced into the wells. The cell proliferation and viability under the cryogels was evaluated by alamarBlue® assay in 24 h, and LIVE/DEAD® Viability/Cytotoxicity Kit assay after 1, 3, and 5 days. The cryogel disks and medium were removed and 10 µL of alamarBlue® reagent in 100 µL complete growth medium was then added into each well. The plate was incubated for 4 h in a humidified incubator containing 5% CO_2 at 37°C. After that, 100 µL of the medium in each well was transferred into a 96-well black plate (Costar). Fluorescence was read using 560 nm as the excitation wavelength and 600 nm as the emission wavelength using a microplate reader

(Molecular Devices) according to the manufacturer's instructions. Cells seeded on TCP without film pieces served as the positive control group. Tests were repeated six times for each group. Cell adhesion and viability were observed under an inverted fluorescence microscope (IX53, Olympus). The cell viability was evaluated by alamarBlue® assay after cultured for 24 h.

For the leaching pattern test, the cryogels were sterilized and air dried, then different concentrations (from 5 to 10, 15 and 20 mg/mL) of cryogels were immersed in the DMEM with a shaking (100 rpm) at 37 °C for 24 h to obtain the extract solutions. L929 cells were seeded in 96-well plate at a density of 10000 cells/well and cultured for 12 h. Then the cryogel extract solutions were used to replace the culture medium and cultured for 24 h. The cell proliferation and viability with cryogel extract solutions was evaluated by LIVE/DEAD® Viability/Cytotoxicity Kit assay after 24 h and the method is consistent with the above test of the direct contact.

In vivo biocompatibility test of the cryogels

The *in vivo* biocompatibility and of all the cryogels were examined by implanting the films under the skin of SD rats. The test cryogels with 8 mm diameter were cut into 5 mm height and sterilized with 75% ethanol, and rinsed in phosphate-buffered saline (PBS) overnight. Subsequently, the sterilized cryogels were implanted under the skin. The implanted cryogels along with their surrounding tissues and skin were retrieved at week 1 and week 4 after implantation. The histomorphological determination of retrieved samples were then observed by hematoxylin-eosin (H&E) staining. The stained slides were observed and analyzed by microscope. All the animal experiments

were performed according to the guidelines established by the committee on animal research at Xi'an Jiaotong University.

Antioxidant efficiency of the cryogels

The antioxidant efficiency of the cryogels were assessed by their scavenging ability of stable DPPH free radical. Briefly, the cryogels were made into homogenate by using tissue grinder. DPPH (3.0 ml, 100 µM) and dispersion of samples (containing 12 mg cryogels) in ethanol was stirred and incubated in a dark place for 30 min, while the conventional ROS scavenger of dopamine (12 mg) to completely remove DPPH was used as a positive control. Then, wavelength scanning was performed using a UV–vis spectrophotometer. The DPPH degradation was calculated using the following equation:

$$DPPH \text{ scavenging } (\%) = (A_B - A_H + A_D)/A_B \times 100\% \tag{S8}$$

where A_B was the absorption of the blank (DPPH + ethanol), A_H was the absorption of the film (DPPH + ethanol + cryogels) and A_D was the absorption of the film (DPPH + ethanol + dopamine).

Antibacterial activity assay of the cryogels

Staphylococcus aureus (S. aureus) (ATCC 29213) and Escherichia coli (E. coli) (ATCC 8739) were employed to test the antibacterial activity of the cryogels. In brief, the cylindrical cryogels with the 8 mm diameter were cut into 3 mm length and sterilized by 75% alcohol. Then the cryogels were placed in the well of a 24-well plate and infiltrated with 200 µL sterilized DPBS. Then 10 µL bacterial suspension (in PBS, 10^5 CFU mL^{-1}) was added onto the surface of cryogel disks. Next, the 24-well plate was incubated in the incubator at 37°C for 4 h. Finally, 2 ml sterilized DPBS was added to

each well to release the surviving bacteria and the suspension was diluted 100 times, then the 10 μL diluent was added to a Petri dish and incubated at 37°C for 24 h. After that, the colony-forming units (CFU) were used to evaluate the antibacterial properties of all cryogels.

10 μL bacterial suspension (in PBS, 10^5 CFU mL^{-1}) was added in 2 ml sterilized DPBS was the control group. The following equation was used to further measure the bacteria killing ratios (BKR) of all samples:

$$BKR (\%) = (B_R-B_S)/B_R \times 100\% \tag{S9}$$

where B_R was the survivor bacterial count of control group and B_S was the survivor bacterial count of sample groups.

Photo-thermal performance of the cryogels

The photo-thermal performance of the cryogels were evaluated by NIR laser (MDL-III-808nm-1000mW, Changchun New Industries Optoelectronics Tech Co., Ltd.) Briefly, the cylindrical full-water cryogels with the 8 mm diameter were cut into 5 mm length which were irradiated by NIR laser at a power density of 1.4 W/cm^2 for 10 min. The temperature changes of cryogels and the heat maps were recorded by infrared (IR) thermal camera. In addition, in order to evaluate the effect of power density on temperature changes of cryogels, the 1.0, 1.4 and 1.8 W/cm^2 power density of NIR laser were also used to assess the temperature change and the heat maps of QCS/PDA2.0 cryogels.

NIR irradiation assisted antibacterial performance of the cryogels

The cryogel QCS/PDA0.5 and QCS/PDA2.0 disks (with a diameter of 8 mm and height

of 5 mm) were sterilized by immersing them in 75% alcohol, and then equilibrated using sterilized DPBS. 10 µL of bacterial suspension in sterilized DPBS (10^8 CFU mL^{-1}) was added onto the surface of the swollen QCS/PDA0.5 and QCS/PDA2.0 disks. After that, the samples were exposed to NIR laser light (808 nm, 1.4 W/cm^2) for different time intervals from 0 to 1, 3, 5 and 10 min, respectively. 10 µL of bacterial suspension (10^8 CFU mL^{-1}) suspended in 200 µL of DPBS was used as a negative control, which was also exposed to NIR laser light (808 nm, 1.4 W/cm^2). After keeping all the groups contacting with bacteria for 10 min, 1 mL of sterilized DPBS was introduced into each well to re-suspend any bacterial survivor. Then, 10 µL of the above resuspension was added onto agar plate, the colony-forming units on the agar plate were calculated after cultured for 18 to 24 h at 37°C. Tests were repeated three times for each group, and the antibacterial efficiency of all samples which was expressed as bacteria killing ratios (BKR) were measured by the following equation:

$$BKR (\%) = (B_R - B_S)/B_R \times 100\% \tag{S10}$$

where B_R was the survivor bacterial count of control group and B_S was the survivor bacterial count of sample groups.

Hemolytic activity test of the cryogels

In the hemolytic activity test of the cryogels, the red blood cells (RBCs) were obtained from rat whole blood by centrifuged at 116×g for 10 min. Then the RBCs were further purified by DPBS washing for 3 times. Finally, the purified RBCs were diluted to 5% (v/v) suspension. In addition, different concentrations (varies from 1250, 2500, 5000 to 10000 µg/mL) of cryogel dispersion liquids were prepared from lyophilized cryogel by

mechanical grinder. Then the cryogel dispersion liquids with 500 µL were gently mixed with 500 µL of 5% (v/v) RBCs suspension in 2 mL centrifuge tube. The mixtures were incubated for 1 h at 37℃, then the RBCs and the most of cryogel particles were removed by centrifugation (116×g) for 10 min, and the small amount of remaining cryogel particles were further exhaustively cleared by centrifuged at 11617×g for 10 min. The absorbance of the final supernatants were read at 540 nm by a microplate reader (Molecular Devices). In this experiment, the DPBS and 0.1% triton were used as the negative and positive control, respectively. The hemolysis percentage of cryogels were calculated by the formula as follows:

Hemolysis percentage (%) = [(Ac–Ab)/(At–Ab)]×100%   (S11)

Where "Ac" means the absorbance of the supernatants in cryogels groups;

"Ab"represented the absorbance of the supernatants in DPBS groups as negative control;

"At" represented the absorbance of the supernatants in triton groups as positive control.

All the above tests were repeated for 5 times.

Whole blood clotting test of the cryogels

The whole blood clotting test of the cryogels was carried out according to previous work.[2, 3] The cryogels were made into cylindrical with 14 mm diameter and cut into 5 mm length. Then the cryogels were compressed into shape-fixed state. The rat recalcified (0.2 M $CaCl_2$, 10 mM) whole blood for 50 µL was dripped onto the cryogel in 2 mL centrifuge tubes, and the tubes were incubated at 37 ℃ for 30 s, 60 s, 90 s and 150 s, respectively. After that, 10 mL of DI water was carefully added into the tubes to release the uncoagulated blood and do not damage the formed blood clots. Finally, the

supernatants in the tubs were removed carefully and detected their absorbance by a microplate reader (Molecular Devices) at 540 nm. Meanwhile, the blood clotting properties of gelatin sponge and gauze were evaluated as the controls, and the reference value according to the absorbance of untreated 50 µL recalcified whole blood were incubated with the same time (negative control). The whole blood clotting properties of the cryogels were evaluated by the following equation:

Blood Clotting Index (BCI) = [(As-Ao)/(An-Ao)] × 100%   (S12)

Where "As" means the absorbance of the supernatants in samples groups;

"An" represented the absorbance of the supernatants of the negative control;

"Ao" represented the absorbance of the DI water.

All the above examinations have 5 replicates.

Tissue adhesion and removable performance of cryogels

The tissue adhesion ability of QCS/PDA2.0 cryogel was assessed by tissue adhesion display and liver adhesion stretching test. In the test of tissue adhesion display, the various biological tissues, including liver, heart, spleen, lung, kidney were taken from SD rat (250g, female) and amputated tail was from mouse. The cylindrical QCS/PDA2.0 cryogels with the 8 mm diameter were cut into 5 mm length and fixed by compression, then the cryogels were covered in the surface of tissue with no pressure. The adhesion between cryogels and tissues could withstand the tissues' weight. Moreover, the tissue adhesion of cryogels is also demonstrated by load-bearing experiments. Briefly, the cylindrical QCS/PDA2.0 cryogel with the 6 mm diameter and 4 cm length and fixed along the length by compression, then the cryogel was covered

in the surface of mouse's skin with no pressure. Finally, the mouse and the weight on the tail lifted by the cryogel. Furthermore, the adhesive strength between QCS/PDA2.0 cryogel and liver was quantitatively evaluated by Electro-Mechanical Universal Testing Machines (MTS). The cylindrical QCS/PDA2.0 cryogels with the 6 mm diameter and 4 cm length and fixed along the length by compression, then two cryogels were covered in the surface of liver's both ends with no pressure. Finally, the adhesive strength between cryogel and liver was measured by Electro-Mechanical Universal Testing Machines (MTS).

The removable performance of cryogels was evaluated by removing cryogels from rat liver and skin surface. Briefly, the cylindrical QCS/PDA2.0 cryogels with the 6 mm diameter and 4 cm length and fixed along the length by compression, then the cryogels were covered in the surface of rat's skin and liver with no pressure. Finally, tweezer was used to remove the cryogels from the tissue surface.

In vivo **hemostatic performance of noncompressible surface wounds by tissue adhesion, blood cells adhesion, enrichment, and activation of the cryogels**

The *in vivo* hemostatic capacity of the lyophilized cryogels was tested by several proven methods in mouse, rat, rabbit and pig. All animal experiments were approved by the animal research committee of Xi'an Jiaotong University.

Mouse-tail amputation model：

The mouse-tail amputation model was used to evaluate the hemostatic capacity of the lyophilized cryogels; the method was reported in previous articles.[2, 3] The mice (Kunming, female, 5-6 week, 32-38 g) were equally divided into eight groups in

randomly. The 10 wt% chloral hydrate (3 ml/kg) was employed to anesthetize all the mice, and the mice were fixed on a surgical corkboard. Then, the tails of all the mice were cut at the half the length by surgical scalpel. After cutting, the tail of the mouse was placed in free to make sure the blood was loosed normally. Then the wound was covered with the pre-weighted shape-fixed cryogels (lyophilized cryogel with height of 8 mm and diameter of 12 mm was compressed as the shape-fixed state) with no pressure, and observe the bleeding of the wound. The bleeding time and blood loss were recorded until the wound stops bleeding. The wounds were covered by gauze or hemostatic sponge with slight pressure were set as positive control. The wound without treatment was used as negative control group. Each group contains 12 mice.

Mouse liver prick injury model:

For mouse liver prick injury model, the mice (Kunming, female, 5-6 week, 32-38 g) were equally divided into eight groups in randomly. The mice were anesthetized by injecting 10 wt% chloral hydrate (3 ml/kg) and fixed on a surgical corkboard. The liver of the mouse was exposed by abdominal incision, and serous fluid around the liver was carefully removed to prevent inaccuracies in the estimation of the blood weight obtained by the hemostatic samples. A pre-weighted filter paper on a paraffin film was placed beneath the liver. Bleeding from the liver was induced using a 16 G needle with the corkboard tilted at about 30°. Then the wound was covered with the pre-weighted shape-fixed cryogels (lyophilized cryogel with height of 8 mm and diameter of 12 mm was compressed as the shape-fixed state) with no pressure, and observe the bleeding of the wound. The bleeding time and blood loss were recorded until the wound stops

bleeding. The wound which was covered by gauze or hemostatic sponge with slight pressure was set as positive control. The wound without treatment was used as negative control group. Each group contains 12 mice.

Standardized circular rabbit liver section model:

The standardized circular rabbit liver section model was used to further evaluate the hemostatic capacity of the lyophilized cryogels in the condition of the large amount of bleeding. The New Zealand White rabbits (male, 1.8-2.0 kg) were fixed on a surgical corkboard and anesthetized by 10 wt% chloral hydrate (5 ml/kg). The liver of the rabbit was exposed by abdominal incision, and serous fluid around the liver was carefully removed to prevent inaccuracies in the estimation of the blood weight obtained by the hemostatic samples. An impermeable film was placed beneath the liver. Then, a standardized circular liver laceration was created by gluing a plastic disc (d = 10 mm) to the surface and superficially excising this area with a blade. After that the wound was covered with the pre-weighted shape-fixed cryogels (lyophilized cryogel with height of 8 mm and diameter of 12 mm was compressed as the shape-fixed state) with no pressure. The blood flowing out was suck out by pre-weight gauze. Then observe the bleeding of the wound, and the bleeding time and blood loss were recorded until the wound stops bleeding. The wounds covered by gauze or hemostatic sponge with slight pressure were set as positive control. The wound without treatment was used as negative control group. Each group contains 8 rabbits.

Pig skin laceration model:

The York pigs (female, ~50 kg) were fixed on surgical table, and an animal anesthesia

machine with isoflurane was employed to anesthetize all the pigs. The wound on pig skin were cut by surgical scalpel into round with 2 cm diameter. After cutting, the skin of the pig was placed in free to make sure the blood was loosed normally. Then the wound was covered with the pre-weighted shape-fixed cryogels (lyophilized cryogel with height of 5 mm and diameter of 3 cm was compressed as the shape-fixed state) with no pressure, and observe the bleeding of the wound. The bleeding time and blood loss were recorded until the wound stops bleeding. The wounds covered by gauze or hemostatic sponge with slight pressure were set as positive control. The wound without treatment was used as negative control group. Each group contains 6 wounds.

In vivo hemostatic performance of surface wounds on coagulopathic hemorrhage model

All animal experiments were approved by the animal research committee of Xi'an Jiaotong University. New Zealand White rabbits (male, 1.8-2.0 kg) were fixed on the surgical cork board and then 10% chloral hydrate was injected into rabbits enterocoelia to anaesthetize them (5 mL/kg). Following that, rivaroxaban solution (2 mg/mL) was prepared in a mixture of PEG400 and water (5:5, v/v) under the help of ultrasound. A desired amount of rivaroxaban solution (300 µg/kg) was administered by intravenous injection. After 3 min, the liver of the rabbit was exposed by an abdominal incision, the serous fluid around the liver was carefully removed, and an impermeable film was placed beneath the liver. The wound in the liver was cut by surgical scalpel for 12 mm with the corkboard tilted at about 30°. Then the wound was covered with the pre-weighted shape-fixed cryogels (lyophilized cryogel with height of 8 mm and diameter

of 12 mm was compressed as the shape-fixed state) with no pressure. The blood flowing out was suck out by pre-weight gauze. Then observe the bleeding of the wound, and the bleeding time and blood loss were recorded until the wound stops bleeding. The wounds covered by gauze or hemostatic sponge with slight pressure were set as positive control. The wound without treatment was used as negative control group. Each group contains 8 rabbits.

In vivo **hemostatic performance of the cryogels on rabbit liver volume defect noncompressible hemorrhage model**

All animal experiments were approved by the animal research committee of Xi'an Jiaotong University. The cylindrical lyophilized cryogel (with diameter of 16 mm and height of 8 mm) was compressed as shape-fixed cylindrical cryogel with the diameter of about 9 mm. Then the shape-fixed cryogel was loaded into syringe (with inner diameter of 9 mm and external diameter of 10 mm) for further *in vivo* injection. Gelatin hemostatic sponges (with a height of 8 mm and diameters of 12 mm) were used as control groups. The New Zealand White rabbits (male, ~2.0 kg) were fixed on the surgical cork board and then 10% chloral hydrate was injected into rabbits enterocoelia to anaesthetize them (5 mL/kg). Following that, the rabbit experienced an abdominal incision to expose its liver, the serous fluid around the liver was carefully removed, and then a columniform liver volume defect (with a diameter of 10 mm and height of 5 mm) was made in right lobe using biopsy needle (inner diameter of 10 mm) and surgical scissors. Immediately after wiping off the blood by using gauze, the cryogel was injected into the defect hole or gelatin hemostatic sponge was inserted into the defect

hole. During the hemostatic process, the weighed gauze was used to absorb the flowing blood. The hemostatic time and blood loss were recorded accordingly. Each group was repeated for 8 times.

***In vivo* wound healing of the cryogels in a full-thickness skin defect model**

The ability of the cryogels to promote wound healing were evaluated by the model of full-thickness skin defect using female Kunming mouse with 5-6-week age and weighting 30-40 g. [4] Our animal experiments were approved by the institutional review board of Xi'an Jiaotong University. Experiments were divided into three groups, including control, CS sponge, and QCS/PDA2.0, each group of 15 mice. All mice were acclimated to the environment for 7 days and anesthetized by intraperitoneal injection of 10% chloral hydrate (3 mL/kg), then hair on mice' back was depilated before surgery. All procedures were performed under aseptic condition and full thickness skin round wounds of 7 mm diameter were created by a needle biopsy during the surgery. After the removal of wound skin, control wounds were dressed with commercial film dressing (Tegaderm™ film), and experiment group wounds were dressed with of QCS/PDA2.0 cryogel (lyophilized cryogel with height of 5 mm and diameter of 10 mm was compressed as the shape-fixed state). On day 5, 10 and 15 after surgery, all tissues around the wound were collected on each 5 mice in 3 groups and were stored at -80°C before analysis. The regeneration process of wounds was assessed by wound area monitoring, histomorphological determination and collagen content detection. For wound area monitoring, on the 5th, 10th, and 15th day, the mice in each group were performed standard anesthesia procedure with intraperitoneal injection of chloral

hydrate (0.3 mg/kg). Then wound area was measured by tracing the wound boundaries on plotting papers.

Wound contraction (%) were calculated using the formula below:

Wound contraction= (area (0 day)-area (n day))/ (area (0 day)) ×100%　　　　　(S13)

Where "n" represents the day of 5th, 10th, and 15th.

For collagen content detection, samples collected on 5th, 10th and 15th day were made into 1 cm^2 square shape and with the same weight, and collagen content was evaluated by commercial kit (Jiancheng Bioengineering, China) to estimate hydroxyproline content. All operations were strictly followed manufacture's instruction.

Histological analysis

In order to evaluate the epidermal regeneration and inflammation in wound area, the collected samples on 5th, 10th, and 15th day were fixed with 4% paraformaldehyde for 1 hour, embedded in paraffin, and then cross sectioned to 4 μm thickness slices. The obtained slices were then stained by Haematoxylin-Eosin (Beyotime, China). All slices were analyzed and photographed by microscope (IX53, Olympus, Japan).

Results

Table S1 The compositions of the cryogels in detail. QCS, DA, SP, and PDA represent quaternized chitosan, dopamine, sodium periodate and polydopamine nanoparticles. The number after PDA represents weight (mg) of polydopamine nanoparticles in per mL cryogel precursor.

Sample	QCS (mg)	DA (mg)	SP (mg)
QCS/PDA0.5	20	0.5	0.564
QCS/PDA1.0	20	1.0	1.128
QCS/PDA2.0	20	2.0	2.256
QCS/PDA3.0	20	3.0	3.384
QCS/PDA4.0	20	4.0	4.512
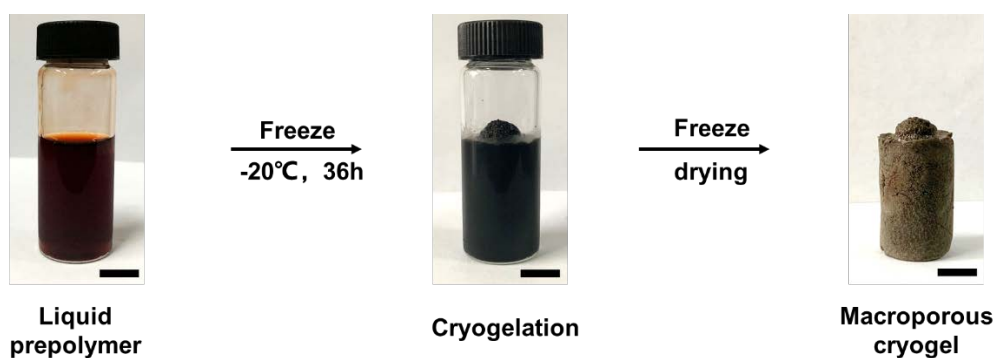
Figure S1. Photographs of the cryogel QCS/PDA2.0 to present the three phases of the cryogel formation.
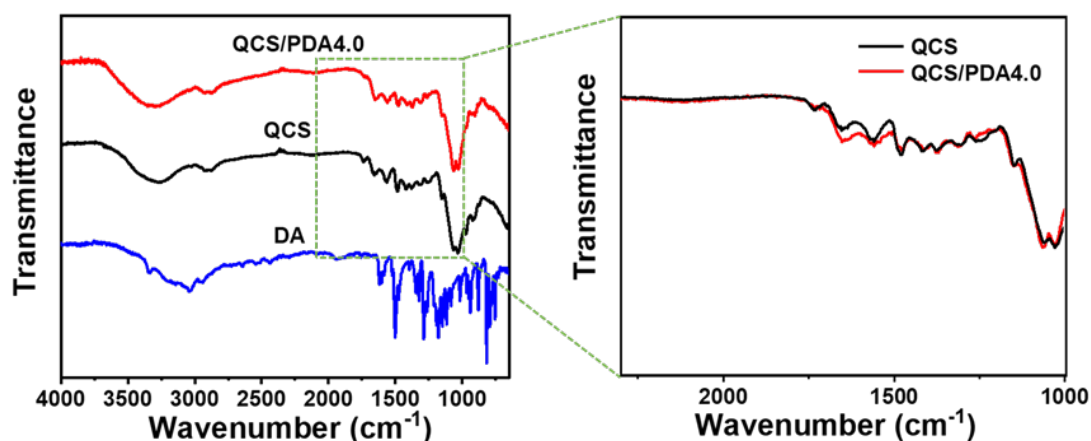
Figure S2. FTIR spectra of dopamine, QCS and dried QCS/PDA2.0 cryogel.

In the spectrum of QCS, two characteristic bands at 1653 and 1559 cm^{-1} were attributed to the CO stretching vibration of –NHCO- and the -NH bending of NH$_2$, respectively.[5] Compared with pure QCS,[5] the spectrum of the QCS/PDA 2.0 cryogel showed almost unchanged NH$_2$ absorption at 1559 cm^{-1} (the amino group introduced by dopamine ≈ the amino group consumed by Schiff base reaction), but the peak enhancement at 1653 cm^{-1} is due to the formation of Schiff base,[6] demonstrating that the o-quinone from dopamine had reacted with the amino groups on the QCS backbone. Moreover, the above conclusion was also proved by XPS.

Table S2. The compositions of the cryogels in the experiment with a suitable

concentration of QCS

Sample	QCS (mg)	DA (mg)	SP (mg)
QCS 1.0 wt%	10	3	3.384
QCS 2.0 wt%	20	3	3.384
QCS 3.0 wt%	30	3	3.384
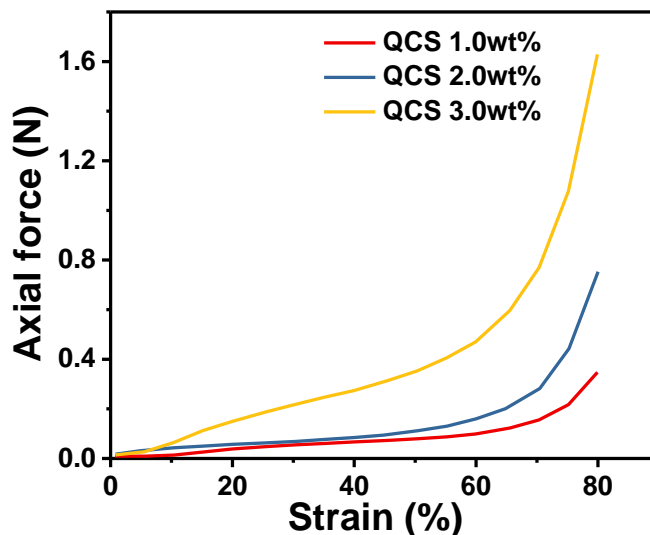
Figure S3. Compression strain of the cryogels with a 3.0 mg/mL constant dopamine concentration and varying the chitosan concentration from 10 to 20 and 30 mg/mL.

In order to choose a suitable concentration of QCS as the basic material of cryogel and the QCS with a concentration higher than 3 wt% is more difficult to dissolve. Therefore, we set the concentration gradient of QCS as 1.0, 2.0, and 3.0 wt% with the same amount of dopamine at 3 mg/mL (Table S2). The obtained cryogel with 1.0 wt% of QCS has too weak mechanical strength, while the mechanical strength of 3.0 wt% QCS cryogel are too excessive. It is fragile when squeezed in wet state and harder to compress in dry state (Figure S3).
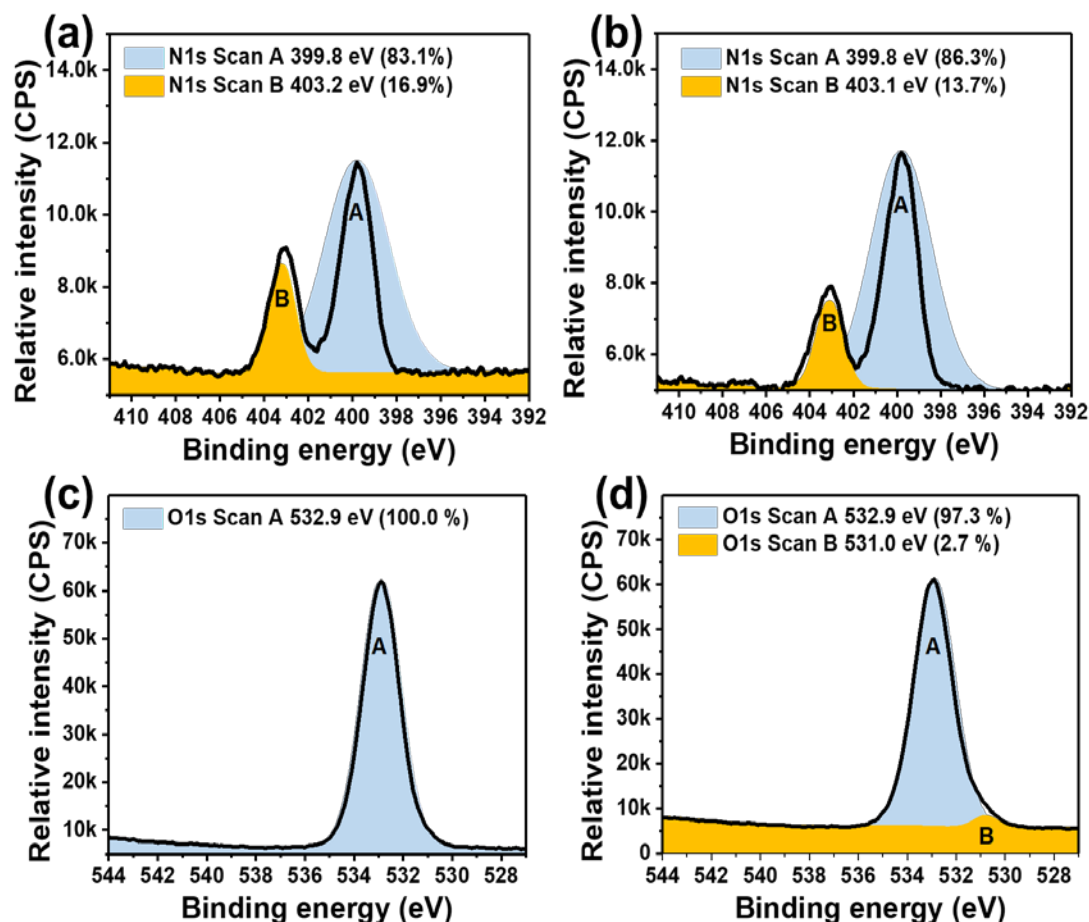
Figure S4. (a) N1s XPS spectra of QCS. (b) N1s XPS spectra of QCS/PDA2.0 cryogel. (c) O1s XPS spectra of QCS. (d) O1s XPS spectra of QCS/PDA2.0 cryogel.

The N1s spectra of QCS and QCS/PDA2.0 were displayed in Figure S4a and Figure S4b. Compared with the N1s spectra of CS with the single peak at 400 eV (100%) in previous report. [7] The spectra of QCS has split into two peaks. One appears at the same binding energy (399.8 eV (83.1%)) as chitosan, and the other new peak at 403.2 eV (16.9%) belongs to the signal from the positively charged nitrogen atom in the quaternary ammonium moiety, which can prove the successful synthesis of QCS. In the spectra of QCS/PDA2.0, the proportion of the 399.8 eV peak was increased from 83.1% to 86.3%, which was attributed to the introduction of the nitrogen atom in polydopamine. As shown in the Figure S4c, the O1s spectra of QCS has one peak at

22

532.9 eV (100%), which belongs to the binding energy of O-H and C-O-C. After the introduction of polydopamine in QCS/PDA2.0, the new O1s peak at 531.0 eV (2.7%) can be regarded as the binding energy of C=O of polydopamine (Figure S4d).
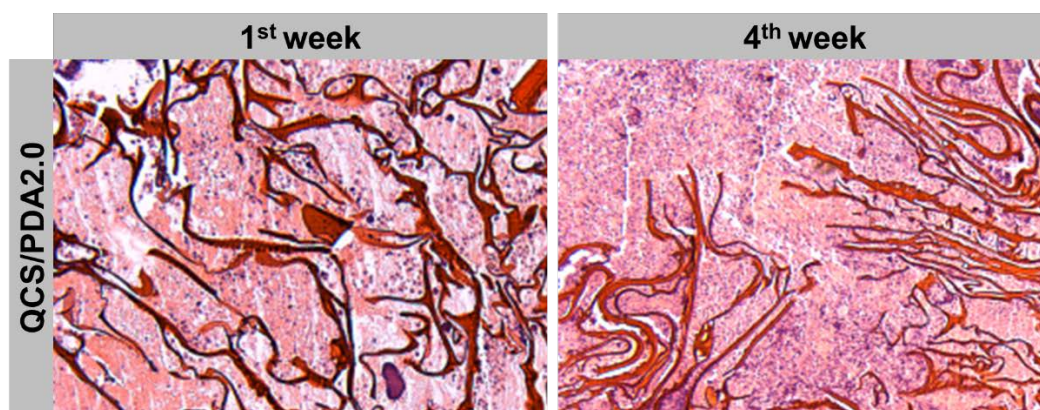
Figure S5. H&E staining results of QCS/PDA2.0 cryogels after 1 week and 4 weeks' implantation. Scale bar: 400 μm.
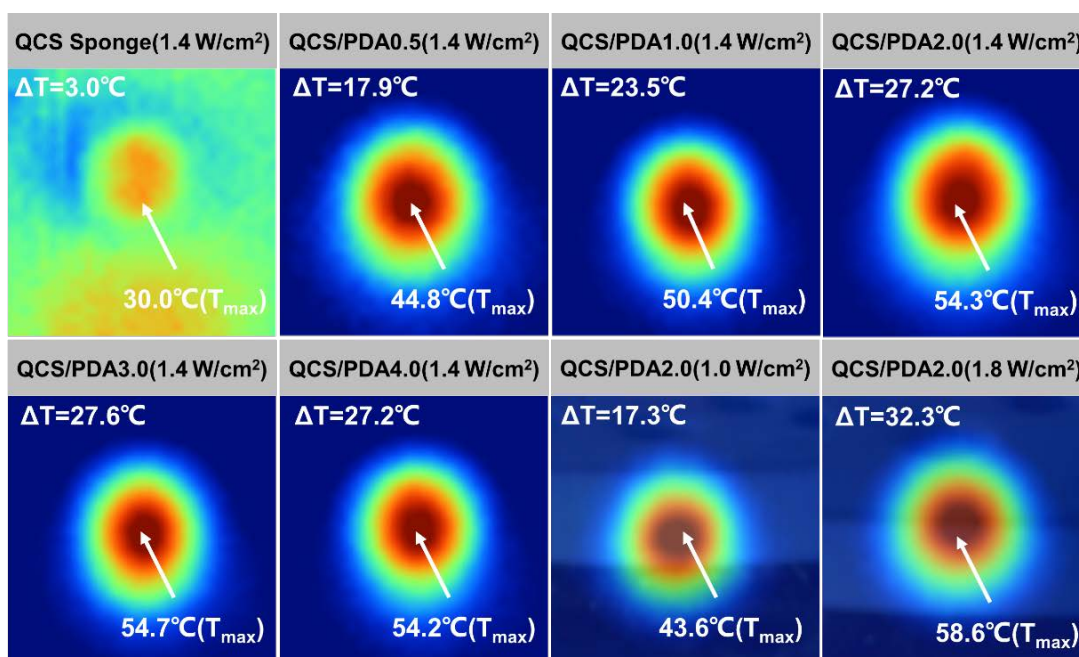

Figure S6. Heat maps of the QCS sponge and all cryogels after 10 min NIR 808 nm irradiation with a constant light intensity of 1.4 W/cm^2; Heat maps of QCS/PDA2.0 after 10 min NIR 808 nm irradiation with the light intensity varying from 1.0 to

1.8W/cm^2.
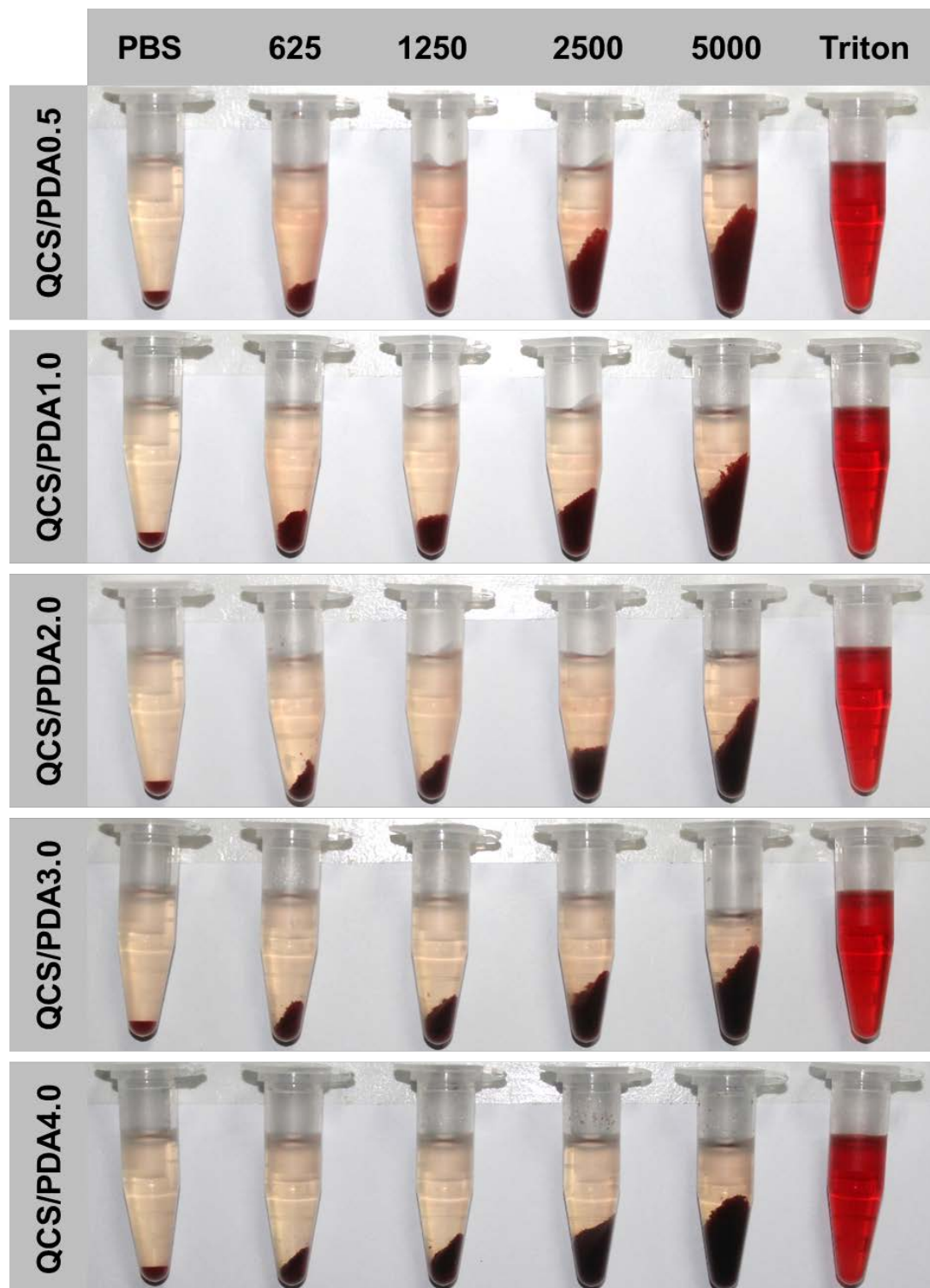
Figure S7. Photographs from hemolytic activity assay of the cryogels using PBS as negative control and Triton X-100 as positive control.
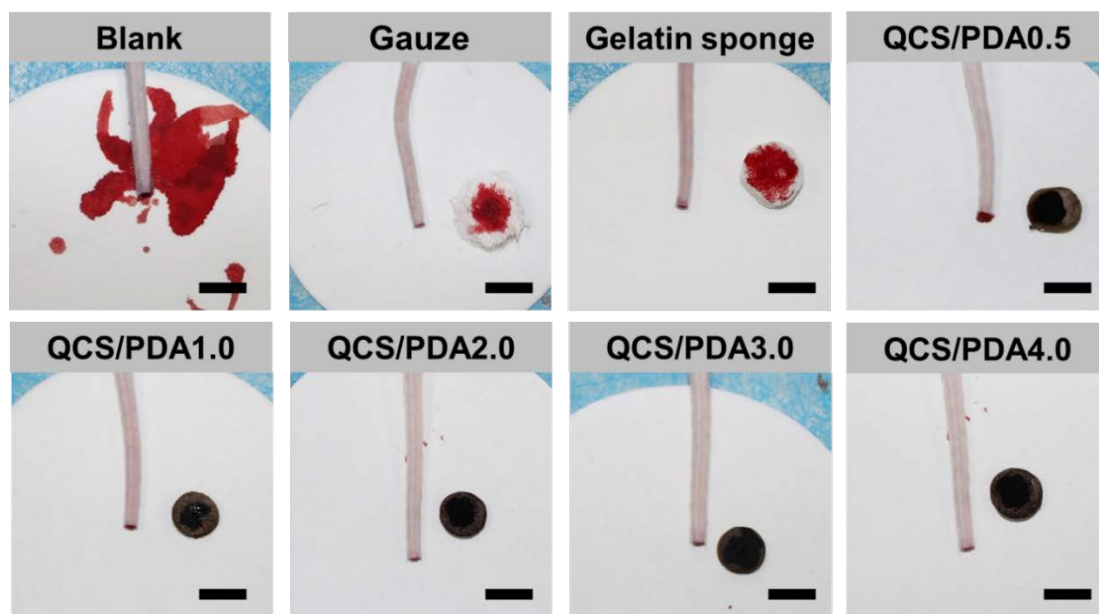
Figure S8. Photographs of the hemostatic agent groups and blank group after *in vivo* hemostasis when used in the mouse-tail amputation model. Scale bar: 12 mm.
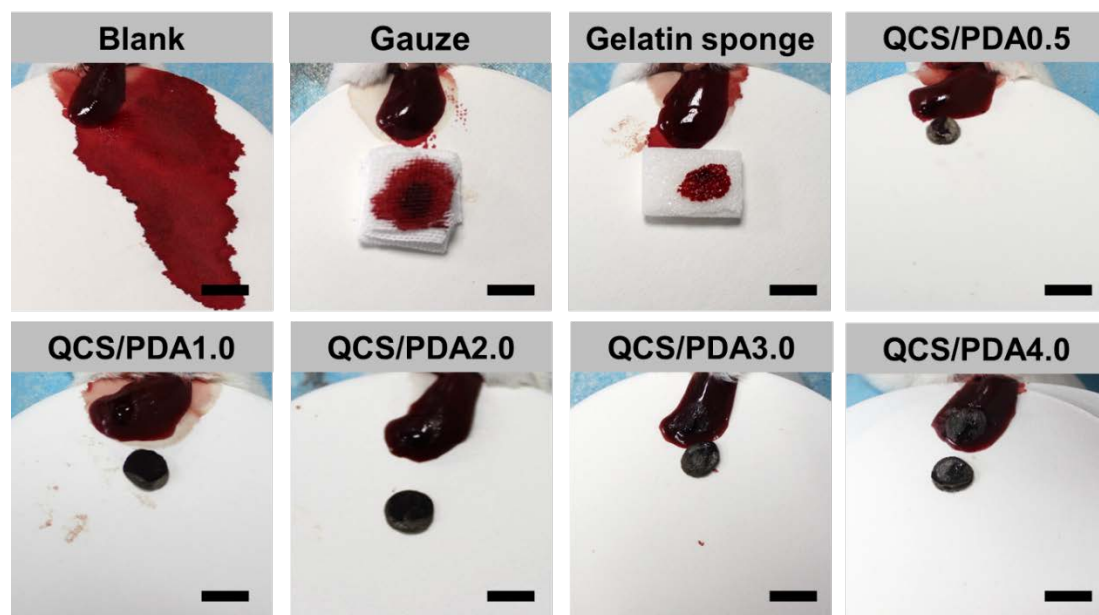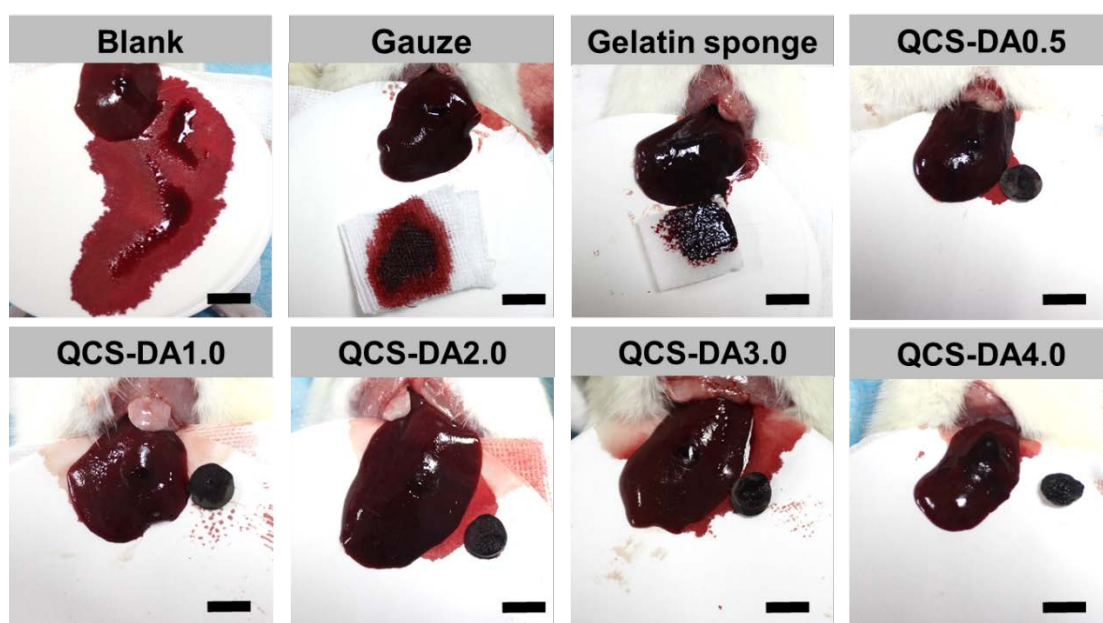

Figure S9. Photographs of the hemostatic agent groups and blank group after *in vivo* hemostasis when used in the mouse liver prick injury model. Scale bar: 12 mm.

Figure S10. Photographs of the hemostatic agent groups and blank group after *in vivo* hemostasis when used in the standardized strip rat liver injury model. Scale bar: 12 mm.
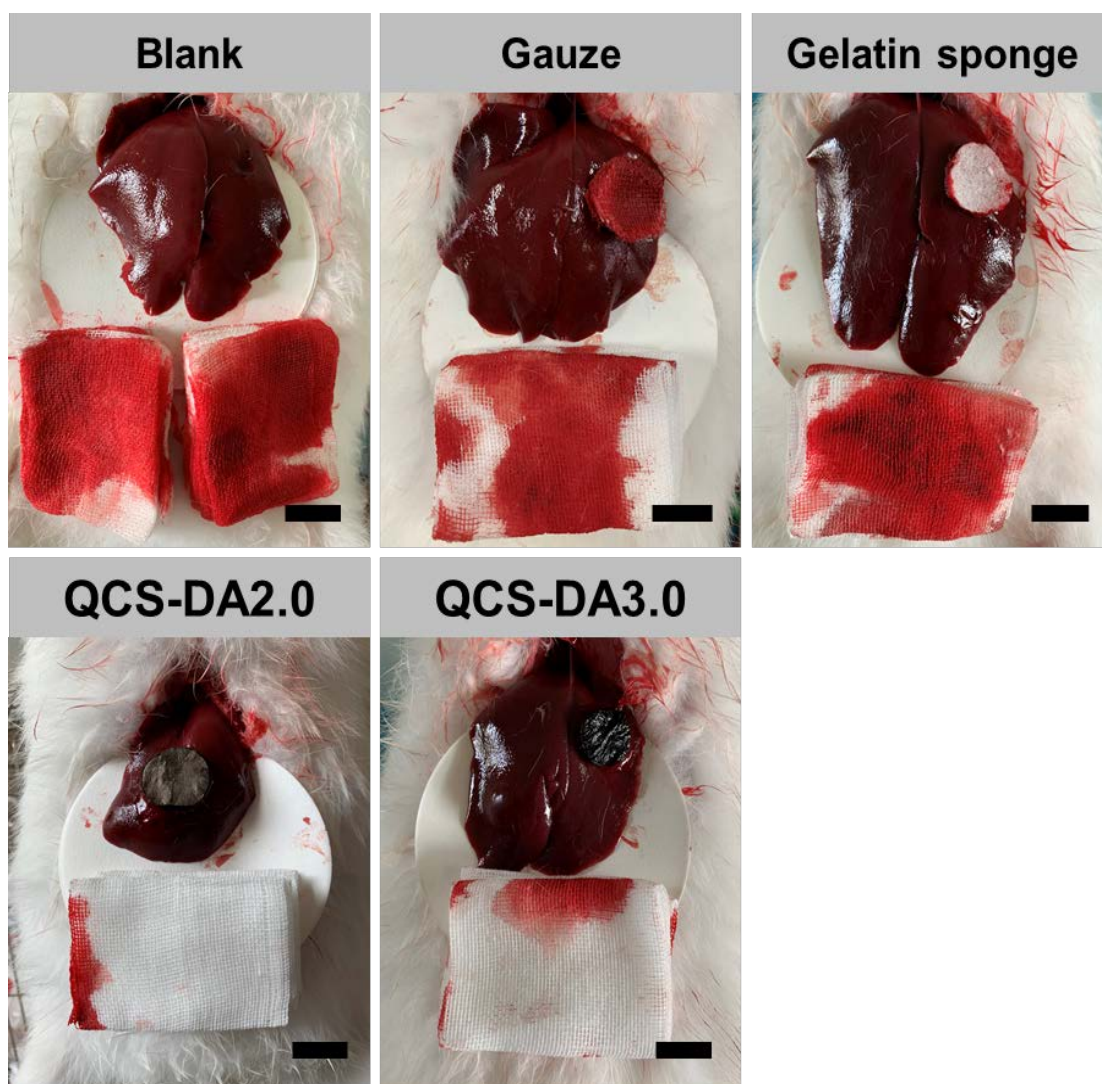
Figure S11. Photographs of the hemostatic agent groups and blank group after in vivo hemostasis when used in standardized circular rabbit liver section model. Scale bar: 20 mm.
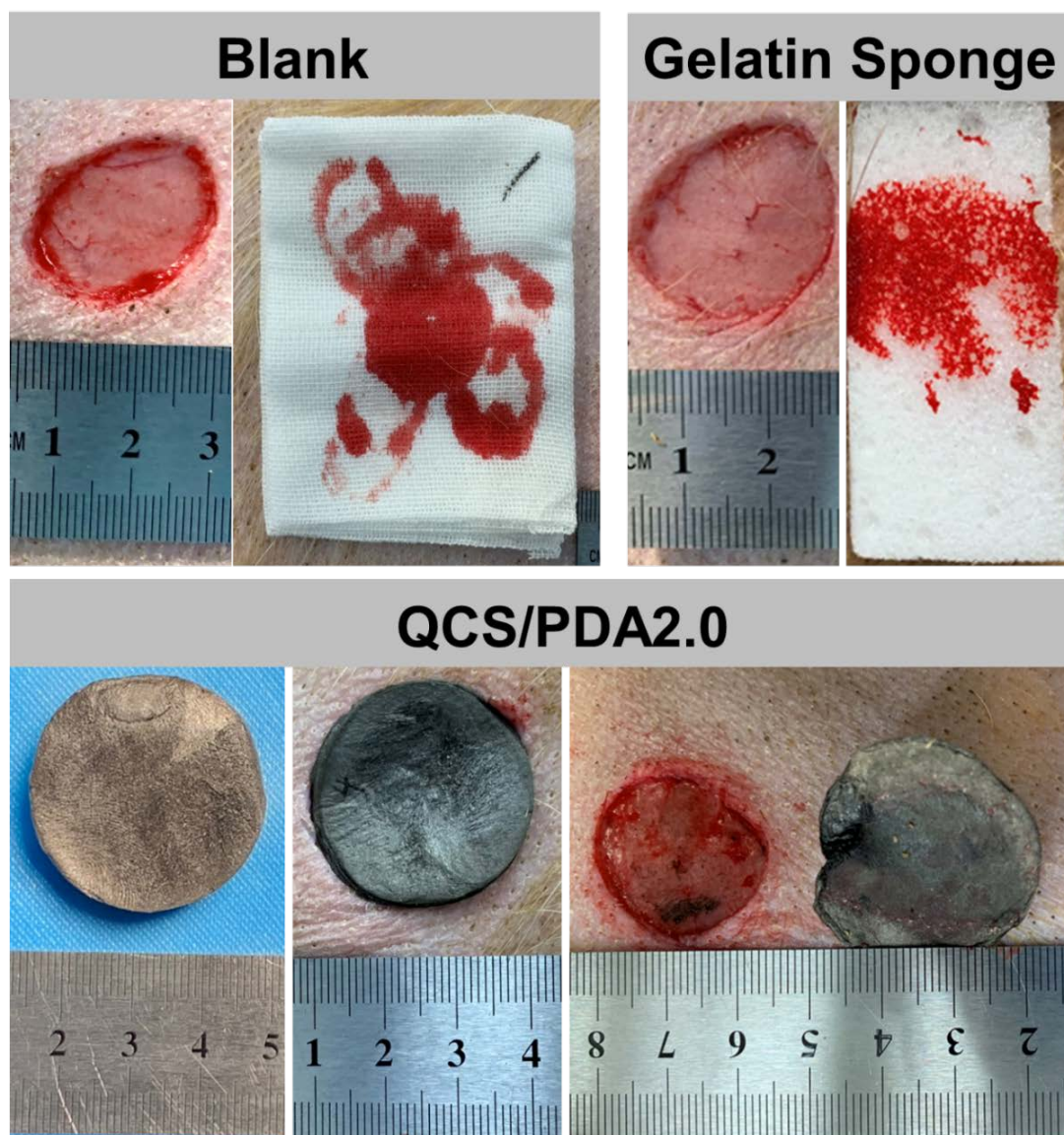
Figure S12. Photographs of the hemostatic agent groups and blank group after in vivo hemostasis when used in the pig skin laceration model.
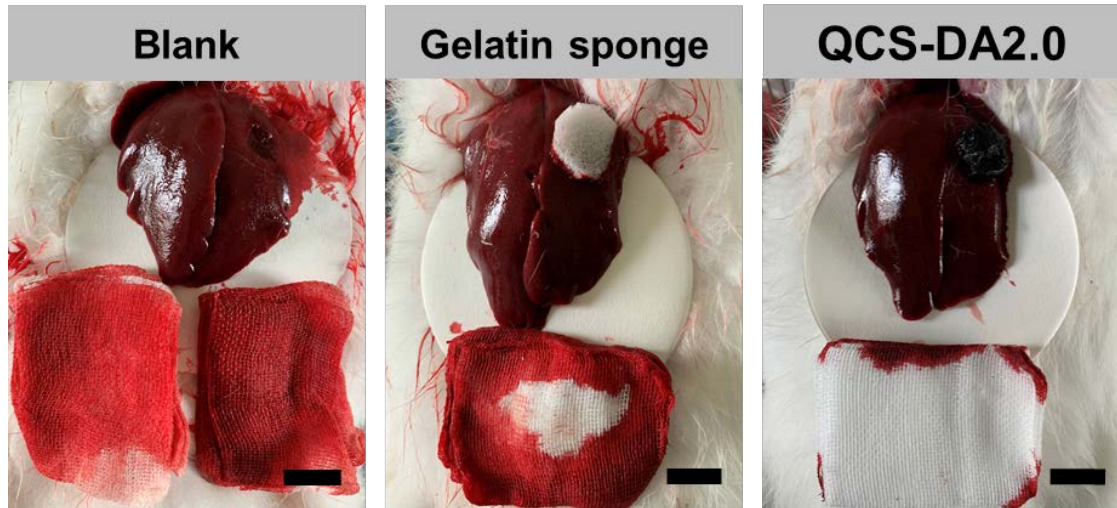
Figure S13. Photographs of the hemostatic agent groups and blank group after in vivo hemostasis when used in coagulation disorder rabbit with standardized circular liver section model. Scale bar: 20 mm.
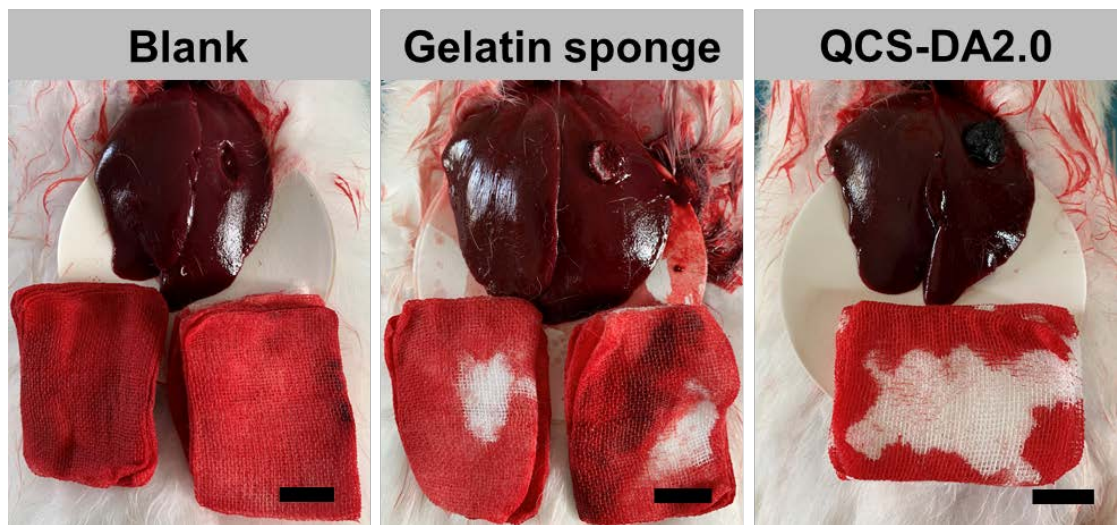

Figure S14. Photographs of the hemostatic agent groups and blank group after in vivo hemostasis when used in the rabbit liver volume defect noncompressible hemorrhage model. Scale bar: 20 mm.

References：

1. Zhao, X.; Li, P.; Guo, B. L.; Ma, P. X., Antibacterial and Conductive Injectable Hydrogels Based on Quaternized Chitosan-Graft-polyaniline/oxidized Dextran for Tissue Engineering. *Acta Biomater.* **2015,** *26*, 236-248.

2. Zhao, X.; Guo, B. L.; Wu, H.; Liang, Y. P.; Ma, P. X., Injectable Antibacterial Conductive Nanocomposite Cryogels with Rapid Shape Recovery for Noncompressible Hemorrhage and Wound Healing. *Nat. Commun.* **2018,** *9*.

3. Quan, K. C.; Li, G. F.; Tao, L.; Xie, Q.; Yuan, Q. P.; Wang, X., Diaminopropionic Acid Reinforced Graphene Sponge and Its Use for Hemostasis. *Acs Appl. Mater. Inter.* **2016,** *8* (12), 7666-7673.

4. Zhao, X.; Wu, H.; Guo, B.; Dong, R.; Qiu, Y.; Ma, P. X., Antibacterial Anti-oxidant Electroactive Injectable Hydrogel as Self-healing Wound Dressing with Hemostasis and Adhesiveness for Cutaneous Wound Healing. *Biomaterials* **2017,** *122*, 34-47.

5. Jing, X.; Mi, H.-Y.; Napiwocki, B. N.; Peng, X.-F.; Turng, L.-S., Mussel-inspired Electroactive Chitosan/graphene Oxide Composite Hydrogel with Rapid Self-healing and Recovery Behavior for Tissue Engineering. *Carbon* **2017,** *125*, 557-570.

6. Zhao, X.; Zhang, M.; Guo, B.; Ma, P. X., Mussel-inspired Injectable Supramolecular and Covalent Bond Crosslinked Hydrogels with Rapid Self-healing and Recovery Properties via a Facile Approach Under Metal-free Conditions. *J. Mater. Chem. B* **2016,** *4* (41), 6644-6651.

7. Vallapa, N.; Wiarachai, O.; Thongchul, N.; Pan, J. S.; Tangpasuthadol, V.; Kiatkamjornwong, S.; Hoven, V. P., Enhancing Antibacterial Activity of Chitosan Surface by Heterogeneous Quaternization. *Carbohyd. Polym.* **2011,** *83* (2), 868-875.